Renal phosphate wasting due to tumor-induced osteomalacia: a frequently delayed diagnosis

M. Odette Gore[1,2], Brian J. Welch[1,2], Weidong Geng[1,2], Wareef Kabbani[3], Naim M. Maalouf[1,2], Joseph E. Zerwekh[1,2], Orson W. Moe[1,2] and Khashayar Sakhaee[1,2]

[1]Charles and Jane Pak Center for Mineral Metabolism and Clinical Research, University of Texas Southwestern Medical Center, Dallas, Texas, USA; [2]Department of Internal Medicine, University of Texas Southwestern Medical Center, Dallas, Texas, USA and [3]Department of Pathology, University of Texas Southwestern Medical Center, Dallas, Texas, USA

CASE PRESENTATION

A 52-year-old white female with a history of profound hypophosphatemia, muscle weakness, and multiple debilitating atraumatic fractures was referred in March 2004 for evaluation at the Mineral Metabolism Clinic. Five years prior, she had sustained bilateral rib fractures which failed to heal. In May 2000, she was diagnosed with primary hyperparathyroidism based on serum calcium of 10.4 mg/dl (reference range 8.4–10.2 mg/dl), parathyroid hormone (PTH) of 97 pg/ml (reference 10–65 pg/ml), phosphorus of 2.0 mg/dl (reference 2.5–4.5 mg/dl), and alkaline phosphatase of 420 IU/l (reference 38–126 IU/l). Bone density measured by dual energy X-ray absorptiometry (DXA) revealed T-scores of −2.9 (lumbar spine) and −3.5 (femoral neck), indicative of osteoporosis. In July 2000, the patient underwent partial parathyroidectomy with removal of two parathyroid glands (histologic diagnosis: adenoma for left superior gland, normal for left inferior gland). Intraoperatively, serum PTH fell from 58 to 13 pg/ml at 24 min post-excision. In the ensuing months, serum calcium normalized, but PTH remained elevated and serum phosphorus remained low. One year after the first parathyroid surgery, the patient underwent a subtotal parathyroidectomy (histologic diagnosis: hyperplasia), leaving only about 20–30 mg of the right inferior gland, and was placed on low dose calcitriol (0.5 μg daily). Over the next three years, she progressively lost mobility due to muscle weakness, requiring assistance in ambulation. She developed multiple additional atraumatic fractures (bilateral superior and inferior pubic ramus, bilateral femoral head, radial neck, ulnar, and multiple vertebral) resulting in kyphosis. After repeated neurological and rheumatological evaluations, she was referred to our clinic. In June 2004, she complained of profound fatigue and severe pain in the low back and thoracic area and required a walker for ambulation. Physical examination revealed a well-nourished kyphotic woman, with a wide-based gait and generalized decreased muscle strength (4/5). An iliac crest bone biopsy and clinical biochemistry evaluation were performed.

BONE BIOPSY

The bone biopsy (Figure 1) revealed a marked increase in osteoid parameters for both cortical and cancellous bone, including osteoid volume (11.9 and 56.1% of total bone volume, for cortical and cancellous bone respectively), osteoid surface (78.9 and 93.6% of total bone surface), and mean osteoid seam width (24 and 31 μm). Mineralized bone volume and mean thickness were reduced in both cortical and cancellous bone. Osteoblastic surfaces were present but reduced for the amount of osteoid present. Resorptive parameters were not increased and frankly low for cancellous bone. Tetracycline labeling was absent in all sections examined, indicating lack of new bone formation. Taken together, these findings are consistent with osteomalacia because of defective bone mineralization.

CLINICAL DIAGNOSIS

The results of the initial clinical biochemistry evaluation, performed during a 4-day constant metabolic diet, are shown in Table 1. In the absence of a family history of hypophosphatemia, the combination of acquired severe hypophosphatemia, renal phosphate wasting, osteomalacia, and inappropriately low 1,25-dihydroxy vitamin D raised the suspicion of tumor-induced osteomalacia (TIO). Consistently, serum fibroblast growth factor 23 (FGF23) measured by enzyme immunosorbent assay directed against the

Correspondence: *Khashayar Sakhaee, Charles and Jane Pak Center for Mineral Metabolism and Clinical Research, University of Texas Southwestern Medical Center, 5323 Harry Hines Boulevard, Dallas, Texas 75390-8885, USA. E-mail: khashayar.sakhaee@utsouthwestern.edu*

Kidney International (2009) **76,** 342–347; doi:10.1038/ki.2008.355; published online 30 July 2008

Received 13 March 2008; revised 1 May 2008; accepted 6 May 2008; published online 30 July 2008

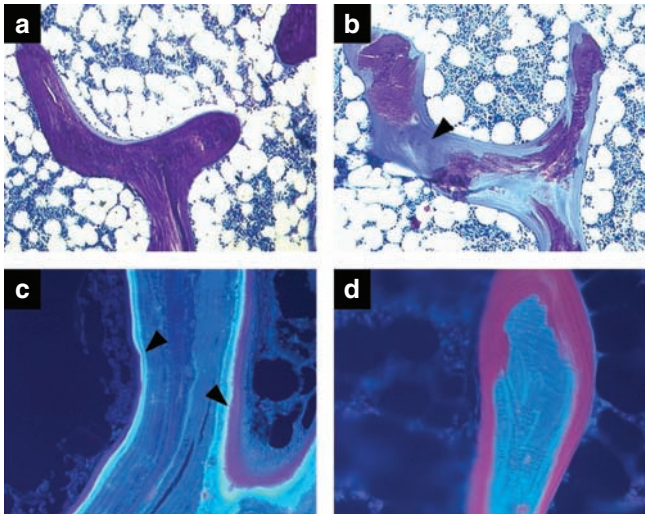

Figure 1 | Histological sections of bone from our patient with tumor-induced osteomalacia (b, d) and from an age- and gender-matched patient with normal bone structure (a, c), used for comparison. (**a**) Normal bone with a very thin layer of osteoid. (**b**) Undercalcified iliac trabecular bone (stained with toluidine blue) is covered by excessive amounts of osteoid (stained light blue, arrow; original magnification $\times 100$). Both cortical and cancellous structural indices of thickness and volume were reduced compared to normal. (**c**) Fluorescence microscopy of bone after double tetracycline labeling shows double fluorescent labels in a patient with normal bone mineralization. (**d**) Tetracycline uptake was severely reduced in the patient as shown by representative trabeculae with no visible label (original magnification $\times 160$). The patient's findings are consistent with a bone mineralization defect (osteomalacia).

Table 1 | Initial metabolic evaluation

Serum calcium	8.5 mg/100 ml	(reference 8.4–10.2 mg/100 ml)
Serum phosphorus	0.7 mg/100 ml	(reference 2.5–4.5 mg/100 ml)
Parathyroid hormone	89 pg/ml	(reference 10–65 pg/ml)
Serum alkaline phosphatase	168 IU/l	(reference 38–126 IU/l)
Serum creatinine	0.7 mg/100 ml	(reference 0.8–1.4 mg/100 ml)
Serum 25-hydroxy vitamin D	30 ng/ml	(reference 5–60 ng/ml)
Serum 1,25-dihydroxy vitamin D	6 pg/ml	(reference 10–65 pg/ml)
Renal fractional excretion of phosphate	40%	
Renal threshold phosphate concentration (TmP/GFR)	0.25–0.30 mg/100 ml	(reference 2.5–4.35 mg/100 ml)
Intestinal calcium absorption (dual-isotope method)	23%	(mean normal 50%)

Laboratory data were collected during a 4-day constant metabolic diet containing 400 mg calcium, 100 mEq sodium, and 800 mg phosphate daily.

C-terminal molecule (Alpco, Salem, NH) was elevated: 573 RU/ml (reference <230 RU/ml). A search for an underlying tumor was initiated. Magnetic resonance imaging of the chest and abdomen had been previously performed and were unremarkable. An ^{111}In-octreotide scintigraphy (octreotide scan) was obtained in September 2004 and revealed an inappropriate focus of uptake slightly to the left of the midline of the head (Figure 2a). Single-photon emission computed tomography revealed an intense focus of radiotracer in the midline, inferior to the cranial vault. Magnetic resonance imaging of the orbit and face demonstrated a $1.5 \times 1.4 \times 1.4$ cm rounded mass within the dorsal aspect of the left nasal cavity (Figure 2b). The mass abutted the dorsal aspect of the inferior nasal turbinate and nasal septum, without invasion of the pterygoid musculature.

While awaiting surgery, in October 2004 the patient was initiated on indomethacin 25 mg, p.o., t.i.d., both for bone pain control and to evaluate the putative effect of indomethacin on FGF23/phosphate metabolism (detailed in Discussion). No significant improvement of hypophosphatemia was noted and indomethacin was discontinued after 4 weeks. The patient was placed on replacement therapy with calcitriol (0.25 μg, p.o., t.i.d.) and phosphate (750 mg, p.o., t.i.d.) until a week before surgery.

A transnasal, endoscopic excision of the nasal mass (Figure 2c) was performed in December 2004. Pathological examination showed diffuse hypercellular spindle cell proliferation arranged in an ill-defined fascicular growth pattern (Figure 3a). The neoplastic cells were mostly short spindled with round to oval nuclei showing mild to moderate cytological atypia (mild hyperchromasia and mild to moderate nuclear pleomorphism). The mitotic rate was low (1–2 per 10 high-power fields). The stroma exhibited prominent capillary-like, thick-walled, and hemangiopericytic-like vessels. Multiple osteoclast-like giant cells (Figure 3b) and focal extracellular mineralized chondroid matrix (Figure 3c) were noted. No necrosis was identified. The pathological diagnosis was phosphaturic mesenchymal tumor, mixed connective tissue variant. Immunohistochemical analysis of paraffin-fixed sections using a monoclonal anti-human FGF23 antibody showed expression of FGF23 protein in the cytoplasm of isolated cells in the excised tumor (Figure 3d–f).

CLINICAL FOLLOW-UP

Figure 4 shows the evolution of markers of phosphate metabolism over 33 months starting from our initial evaluation, including 27 months post-surgery. Postoperative clinical improvement and normalization of biochemical abnormalities confirmed the initial diagnosis of TIO. Serum phosphorus normalized within 1 week after tumor removal. A rapid decrease in serum calcium (to 7.5 mg/100 ml within 24 h) prompted concern of hungry bone syndrome, and further hypocalcemia was prevented with temporary calcium supplementation. Serum 1,25-dihydroxy vitamin D levels normalized 24 h post-intervention, became elevated after 1 week (101 pg/ml), likely because of an abrupt increase in bone mineralization (Figure 4d), and returned to normal 3 months postoperatively. At that time, intestinal calcium absorption measured by dual isotope was increased (77%). Repeat octreotide scan 5 months post-intervention

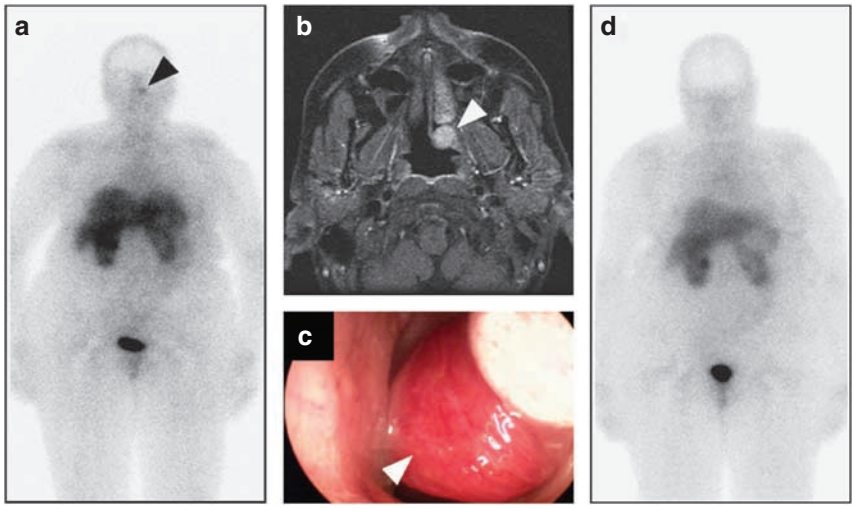

Figure 2 | Radiographic and macroscopic findings. (**a**) ^{111}In-octreotide scintigraphy 3 months before surgery, demonstrating a focus of enhanced inappropriate uptake slightly to the left of the midline of the head (arrow). (**b**) Magnetic resonance imaging of the head shows a 1.5 × 1.4 × 1.4 cm rounded mass (arrow) within the dorsal aspect of the left nasal cavity. (**c**) Macroscopic image of the very vascular tumor *in situ*, just before surgical removal. (**d**) ^{111}In-octreotide scintigraphy 5 months post-surgery, demonstrating lack of tracer uptake in the former location of the tumor.

demonstrated no abnormal tracer uptake (Figure 2d). Bone density at the lumbar spine measured by dual-energy X-ray absorptiometry 6 months after surgery showed a 21% improvement. During 27 months of postoperative follow-up, the patient's clinical complaints of bone pain and muscle weakness progressively resolved, and self-ambulation was restored.

DISCUSSION

TIO is a rare paraneoplastic syndrome characterized by renal phosphate wasting, hypophosphatemia, inappropriately normal or low serum 1,25-dihydroxy vitamin D, and inadequate bone mineralization.[1,2] The clinical manifestations of TIO include fatigue, muscle weakness, bone pain (that can mimic joint pain), and insufficiency fractures ('spontaneous' fractures, caused by physiological levels of mechanical stress exerted upon weakened bone), in the absence of a family history of renal phosphate wasting and/or bone disorders. Disease progress can be slow and insidious, mimicking other rheumatological, neurological, or endocrine disorders, and thus correct diagnosis can be delayed for years or missed altogether. Without intervention, patients become progressively debilitated, experience a markedly decreased quality of life, and are at risk of life-threatening complications. Identification and surgical removal of the offending tumor followed by normalization of phosphate metabolism provides both definitive diagnosis and cure of TIO.

Phosphorus homeostasis

Phosphorus homeostasis is maintained by the interplay between net intestinal absorption, tissue and bone turnover, and renal excretion, with net intestinal absorption matching renal excretion under balance conditions. The kidney assumes a pivotal role in maintaining total body phosphorus balance. Phosphorus circulating as unbound phosphate is freely filtered at the glomerulus and reabsorbed primarily across the proximal tubule. Renal reabsorption of phosphate is regulated by multiple humoral factors, including a class of incompletely understood circulating phosphaturic factors collectively called phosphatonins.[3–6] These were initially discovered as humoral factors secreted by the tumors of patients with TIO, and include FGF23, FGF7, matrix extracellular phosphoglycoprotein, and secreted frizzled-related protein 4. Phosphatonins downregulate renal phosphate reabsorption at least in part by decreasing the abundance of apical sodium/phosphate co-transporters (NaPi-IIa) in the proximal tubule.[6] FGF23 is the most studied phosphatonin, and has a causative role in the pathogenesis of hereditary hypophosphatemias—X-linked hypophosphatemic rickets (XLHR) and autosomal dominant hypophosphatemic rickets—as well as in some cases of acquired hypophosphatemia from TIO.[7,8]

Etiology of hypophosphatemia

Hypophosphatemia can be caused by inadequate dietary intake, decreased intestinal absorption, excessive urinary excretion, or the shift of phosphate from serum into cells and/or bone. Inappropriately high excretion (renal wasting) of phosphate occurs in various genetic and acquired disorders. One common cause is hyperparathyroidism, which is usually associated with moderate hypophosphatemia. Parathyroid hormone (PTH)-independent renal phosphate wasting is usually more severe and may occur because of intrinsic proximal tubular defects (Fanconi syndrome), or because of increased production and/or decreased degradation of phosphatonins. Phosphatonin-related disorders may in turn be genetic (XLHR, autosomal dominant hypophosphatemic rickets, fibrous dysplasia), or acquired (TIO).

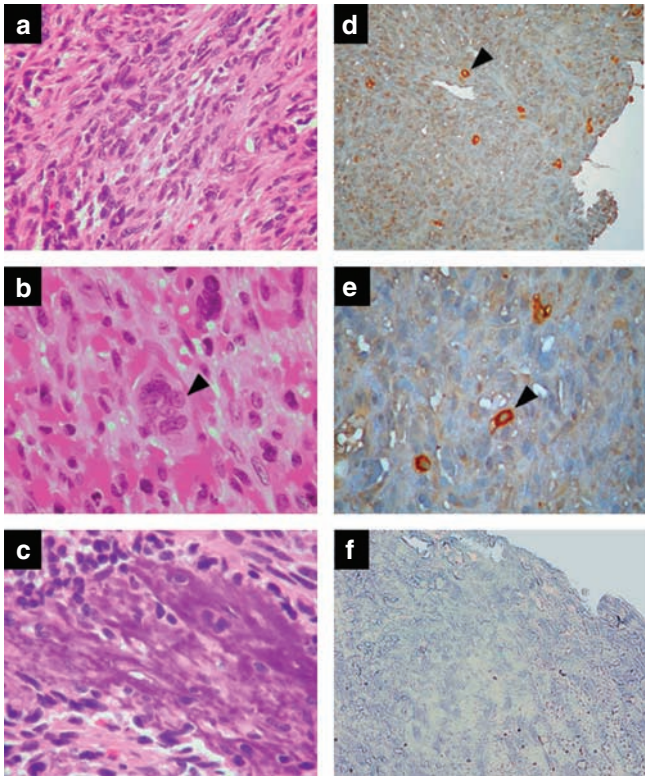

Figure 3 | Histological and immunohistochemical analysis of paraffin-fixed tumor sections. (**a**–**c**) Hematoxylin and eosin staining showing (**a**) sinonasal mucosa with underlying solid proliferation of short spindle and oval cells with bland euchromatic nuclei and with no mitoses easily noted, (**b**) osteoclast-like giant cells (arrowhead), and (**c**) focal mineralized extracellular matrix. (**d**, **e**: original magnification $\times 100$ and $\times 400$) Staining with a monoclonal anti-human FGF23 antibody (R&D Systems, Minneapolis, MN) and a labeled streptavidin-biotin chromogen detection system (IHC kit, Biochain, Hayward, CA). Sections were counterstained with Mayer's Hematoxylin (Volu-Sol, Salt Lake City, UT). FGF23 was expressed in the cytosol of isolated cells (in brown, arrowheads). No staining was observed when the anti-human FGF23 antibody was omitted (**f**, negative control).

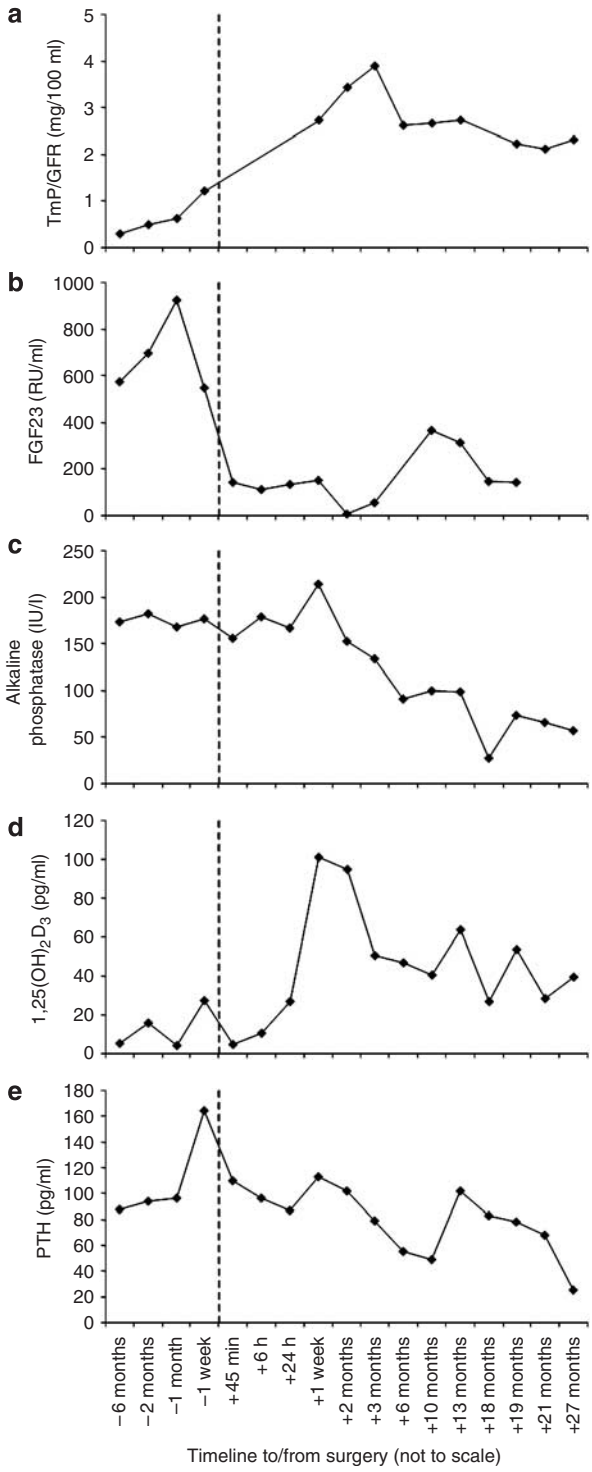

Figure 4 | Biochemical markers of phosphate metabolism pre- and post-surgery. The time of surgery is represented by the dashed line. (**a**) Renal threshold phosphate concentration TmP/GFR. (**b**) Serum FGF23. (**c**) Serum alkaline phosphatase. (**d**) Serum 1,25-dihydroxy vitamin D. (**e**) Serum parathyroid hormone.

Of note, secondary hyperparathyroidism and tertiary hyperparathyroidism have been observed in patients with XLHR and TIO[9,10] and may further contribute to phosphate loss in these patients. The mechanism for this is uncertain, but may be related to reduced 1,25-dihydroxy vitamin D levels leading to decreased intestinal absorption of calcium, hypocalcemia, and consequent upregulation of PTH secretion. Hyperparathyroidism in our patient was initially diagnosed as primary, but in retrospect it is reasonable to suggest that it was actually secondary or tertiary.

Evaluation of hypophosphatemia

Understanding the mechanism of hypophosphatemia is critical for correct diagnosis. Renal phosphate wasting, a hallmark of TIO, should be investigated in any patient with persistent hypophosphatemia. Determination of phosphate clearance and fractional excretion of phosphate do not distinguish true renal phosphate wasting (inappropriate reabsorption from the glomerular filtrate) from other causes of abnormally elevated phosphate excretion (increased net renal inflow of phosphate and/or increased glomerular filtration rate (GFR), exceeding a normal reabsorptive

capacity). Renal wasting can be confirmed by using the nomogram of Walton and Bijvoet[11] to derive renal threshold phosphate concentration (TmP/GFR) from serum phosphorus and tubular reabsorption of phosphate (TRP = 1–phosphate clearance/creatinine clearance, using fasting urine and serum phosphate and creatinine). A low TmP/GFR in spite of hypophosphatemia is indicative of renal phosphate wasting.

The role of FGF23

If FGF23 is markedly increased in the absence of a family history of hypophosphatemia, TIO is likely—although approximately 20% of XLHR cases are because of sporadic mutations and thus have a similar presentation.[12] However, a normal FGF23 level does not exclude TIO, as other tumor-secreted phosphatonins may be involved and are not measured. FGF23 was likely the offending phosphatonin in our case, as FGF23 protein was expressed in the excised tumor (Figure 3d–f), and serum FGF23 normalized after surgery (Figure 4b).

Tumor localization

A search for an underlying tumor should be initiated as soon as the clinical and biochemical findings indicate that TIO is likely. Various tumor locations have been described, including distal extremities, and, most commonly, the nasopharynx and sinuses. Plain radiographs, computed tomography, magnetic resonance imaging, and even positron-emission tomography scanning have been successfully used to localize TIO tumors, and computed-tomography-guided fine-needle biopsy of the tumor has been used to aid in diagnosis. When other imaging techniques fail to identify the tumor (as was the case in our patient), octreotide scan should be considered.[13,14] This technique has high specificity but a negative octreotide scan does not exclude TIO, as some but not all TIO tumors have surface somatostatin receptors. Selective venous sampling for FGF23 has also been successfully used to localize FGF23-secreting tumors.[15,16]

Histopathology

Most tumors associated with TIO are slow-growing, benign, polymorphous neoplasms of mesenchymal origin, classified as osteoblastoma-like, ossifying fibrous-like, non-ossifying fibrous-like, and phosphaturic mesenchymal tumor, mixed connective tissue variant.[17] Of these, phosphaturic mesenchymal tumor, mixed connective tissue variant is the most common, and contains characteristic spindle-shaped neoplastic cells with low or absent mitotic activity in a matrix with calcifications, osteoclast-like giant cells, and rich microvasculature.[18] Rarely, TIO can result from neurofibromatosis, fibrous dysplasia of bone, carcinomas, or metastases.[17,18]

Treatment

Complete removal of the underlying tumor (and thus removal of the source of excess circulating phosphatonins) is to date the only definitive treatment. In most cases this involves surgical resection, but successful computed-tomography-guided radiofrequency ablation of a TIO tumor has also been reported.[19] Before surgery or in nonexcisable tumors (failed localization or surgical contraindication), aggressive phosphate and calcitriol replacement can improve the symptoms, normalize serum phosphorus, but does not improve renal phosphate wasting. Treatment with unlabeled octreotide was attempted with mixed results in patients with somatostatin receptor-positive tumors (as established by radiolabeled octreotide scan).[20,21]

Effect of indomethacin

The therapeutic trial with indomethacin in our patient was prompted by previous findings in hyp mice. The hyp mouse is a murine model of XLHR with decreased FGF23 degradation and increased urinary prostaglandin E2 excretion. Treatment with indomethacin led to amelioration of hypophosphatemia and fractional excretion of phosphate in these mice, without changes in GFR.[22] To our knowledge, this intervention has not been attempted in humans with renal phosphate wasting. The lack of improvement in our patient may be because of insufficient dosage (a higher dose is however not recommended), or because of inherent differences between human TIO and the hyp mouse model.

SUMMARY

In our patient, TIO remained undiagnosed for several years. Careful metabolic evaluation and extensive investigations eventually led to the diagnosis, and TIO was cured by surgical removal of the offending tumor. We emphasize the importance of determining serum phosphorus and TmP/GFR and considering TIO early in the differential diagnosis of unexplained persistent bone pain, apparent joint pain, muscle weakness, and spontaneous fractures.

ACKNOWLEDGMENTS

This work was supported by the National Institutes of Health grants P01-DK20543 and M01-RR00633.

REFERENCES

1. Drezner MK. Tumor-induced osteomalacia. *Rev Endocr Metab Disord* 2001; **2**: 175–186.
2. Kumar R. Tumor-induced osteomalacia and the regulation of phosphate homeostasis. *Bone* 2000; **27**: 333–338.
3. Schiavi SC, Moe OW. Phosphatonins: a new class of phosphate-regulating proteins. *Curr Opin Nephrol Hypertens* 2002; **11**: 423–430.
4. Quarles LD. FGF23, PHEX, and MEPE regulation of phosphate homeostasis and skeletal mineralization. *Am J Physiol Endocrinol Metab* 2003; **285**: E1–E9.
5. Schiavi SC, Kumar R. The phosphatonin pathway: new insights in phosphate homeostasis. *Kidney Int* 2004; **65**: 1–14.
6. Berndt TJ, Schiavi S, Kumar R. 'Phosphatonins' and the regulation of phosphorus homeostasis. *Am J Physiol Renal Physiol* 2005; **289**: F1170–F1182.
7. Shimada T, Mizutani S, Muto T *et al.* Cloning and characterization of FGF23 as a causative factor of tumor-induced osteomalacia. *Proc Natl Acad Sci* 2001; **98**: 6500–6505.
8. Stubbs J, Liu S, Quarles LD. Role of fibroblast growth factor 23 in phosphate homeostasis and pathogenesis of disordered mineral metabolism in chronic kidney disease. *Semi Dial* 2007; **20**: 302–308.

9. Huang QL, Feig DS, Blackstein ME. Development of tertiary hyperparathyroidism after phosphate supplementation in oncogenic osteomalacia. *J Endocrinol Invest* 2000; **23**: 263–267.
10. Savio RM, Gosnell JE, Posen S *et al.* Parathyroidectomy for tertiary hyperparathyroidism associated with X-linked dominant hypophosphatemic rickets. *Arch Surg* 2004; **139**: 218–222.
11. Walton RJ, Bijvoet OLM. Nomogram for derivation of renal threshold phosphate concentration. *Lancet* 1975; **306**: 309–310.
12. Dixon PH, Christie PT, Wooding C *et al.* Mutational analysis of PHEX gene in X-linked hypophosphatemia. *J Clin Endocrinol Metab* 1998; **83**: 3615–3623.
13. Jan de Beur SM, Streeten EA, Civelek AC *et al.* Localisation of mesenchymal tumours by somatostatin receptor imaging. *Lancet* 2002; **359**: 761–763.
14. Nguyen BD, Wang EA. Indium-111 pentetreotide scintigraphy of mesenchymal tumor with oncogenic osteomalacia. *Clin Nucl Med* 1999; **24**: 130–131.
15. Takeuchi Y, Suzuki H, Ogura S *et al.* Venous sampling for fibroblast growth factor-23 confirms preoperative diagnosis of tumor-induced osteomalacia. *J Clin Endocrinol Metab* 2004; **89**: 3979–3982.
16. van Boekel G, Ruinemans-Koerts J, Joosten F *et al.* Tumor producing fibroblast growth factor 23 localized by two-staged venous sampling. *Eur J Endocrinol* 2008; **158**: 431–437.
17. Jan de Beur SM. Tumor-induced osteomalacia. *JAMA* 2005; **294**: 1260–1267.
18. Folpe AL, Fanburg-Smith JC, Billings SD *et al.* Most osteomalacia-associated mesenchymal tumors are a single histopathologic entity: an analysis of 32 cases and a comprehensive review of the literature. *Am J Surg Pathol* 2004; **28**: 1–30.
19. Hesse E, Rosenthal H, Bastian L. Radiofrequency ablation of a tumor causing oncogenic osteomalacia. *N Engl J Med* 2007; **357**: 422–424.
20. Paglia F, Dionisi S, Minisola S. Octreotide for tumor-induced osteomalacia. *N Engl J Med* 2002; **346**: 1748–1749.
21. Seufert J, Ebert K, Muller J *et al.* Octreotide therapy for tumor-induced osteomalacia. *N Engl J Med* 2001; **345**: 1883–1888.
22. Baum M, Loleh S, Saini N *et al.* Correction of proximal tubule phosphate transport defect in Hyp mice *in vivo* and *in vitro* with indomethacin. *Proc Natl Acad Sci USA* 2003; **100**: 11098–11103.